Pion valence structure at intermediate x in the residual-field approach

Joseph Maerovitz and Misak Sargsian
Florida International University, Miami, Florida 33199, USA

Christopher Leon
Los Alamos National Laboratory, Los Alamos, New Mexico 87545, USA

(Received 18 March 2026; revised 12 August 2026; accepted 29 September 2026; published 28 October 2026)

We calculate the valence parton distribution function (PDF) of pion within the theoretical approach based on spectral function representation of valence quarks in the pion. In this approach we assume that the soft partonic structure of pion is defined by the valence $q\bar{q}$ cluster, consisting of current quarks, embedded in the residual field of the pion. The valence PDF is calculated using phenomenological light-front wave functions for the $q\bar{q}$ cluster and the residual field. Our result indicates that the peak position of the x weighted valence PDF (xPDF) depends on parameters characterizing the virtuality of the valence quark cluster and the mass of the residual system. Magnitudes of these parameters are obtained by fitting to the height and the peak position of empirical pion xPDF evaluated at starting Q_0. They indicate that unlike the nucleon case, very little residual mass is needed to describe existing pion PDFs at intermediate x. They also indicate that the $q\bar{q}$ cluster is highly virtual and on average the interacting quark carries almost all of the momentum of the $q\bar{q}$ cluster. This picture is consistent with the dominance of the Feynman mechanism leaving little room for the hard component in the PDF and practically describing $\approx (1-x)$ behavior observed recently at $x \to 1$ limit. Our nontrivial observation is that the height and the peak position of xPDF define the analytic behavior of valence PDF at $x \to 1$ limit.

DOI: 10.1103/tsgs-hj99

I. INTRODUCTION

As the lightest hadron and a pseudo-Goldstone boson of chiral symmetry breaking, the pion holds a unique position in hadronic and nuclear physics. Studying its structure is essential for understanding the nature of the strong interaction of nucleons which in part is mediated through the pion exchange.

While in the chiral symmetry breaking picture the long range part of the nucleon-nucleon (NN) interaction is mediated through the near-massless Goldstone field without apparent internal structure of pion, the deep-inelastic scattering from pion indicates its underlying quark-gluon structure which does not reveal itself in NN interaction. This apparent duality indicates on possible specific distribution of valence quarks in the pion that makes for example the quark interchange in NN interaction through the pion field highly unlikely.

One of the important quantities that allows to explore the dynamical structure of pion is its parton distribution function (PDF) probed at the light-front momentum fraction, x ($0 < x < 1$) and given resolution Q^2. It allows us to probe valence and sea quarks as well as gluon distributions which dominate at different regions of x in the pion.

For the valence quarks pion represents the simplest system and as such it is the best testing ground for understanding the nonperturbative quantum chromodynamics (QCD) mechanism of valence quark distribution in the hadron, thus attracting multitude of theoretical studies ranging from the Nambu–Jona-Lasinio model [1], QCD sum rules [2–4], light-front approaches [5–10], light-front approaches with anti-de Sitter (AdS)/QCD correspondence [11], the appraach based on Dyson-Schwinger equations [12,13] as well as lattice calculations [14]. Other approaches were based on construction of effective Hamiltonian with the holographic QCD confinement potential and Nambu–Jonaa-Lasino interaction [15]

Much progress has been made in the experimental extraction of pion parton distribution exploring variety of deep-inelastic reactions including Drell-Yan, J/Ψ- production, and Sullivan processes (see, e.g., [16–25]).

The recent high quality combined analysis of Drell-Yan and Sullivan processes [24,25] produced an unexpected result for parton distribution functions (PDFs) at large x, observing a behavior of $(1-x)^\beta$ with $\beta \approx 1 - 1.2$. This contradicts to the generally expected dependence of $(1-x)^2$ which in part follows from the expectation that high x parton distributions are generated through the hard gluon exchange between valence quarks [26–28].

Focusing on the dynamics of valence quark distribution in hadrons, we notice two important properties of valence quarks that will be used in our calculation. The first is that

Published by the American Physical Society under the terms of the Creative Commons Attribution 4.0 International license. Further distribution of this work must maintain attribution to the author(s) and the published article's title, journal citation, and DOI. Funded by SCOAP³.

the valence quarks define quantum numbers of hadrons and their flavor is conserved. As such they can be considered as effective fermions whose number is conserved. The second prominent feature of valence quarks is that their distribution weighted by the momentum fraction x, $xf_V(x)$ shows a distinctive peak associated with the average momentum fraction carried by valence quarks. In general, such a peaking property in Fermi systems is associated with the "bulk" property of bound system which has an inherently nonperturbative character. In our recent works [29,30] on modeling valence quark distributions in the nucleon the "bulk" property of hadrons have been described through the quark-gluon system residual to the valence quarks in the nucleon. The model is based on residual mean field approximation which introduces the light-front wave function of the valence quark cluster embedded in the interacting residual field. Introducing a residual field in the description of partonic dynamics of the hadron, which is characterized by its mass and energy, theoretically corresponds to the spectral function approach in the description of the composite bound system. As such this approach is different from commonly considered theoretical approaches in which valence quarks are the entities that fully describe the partonic dynamics in the intermediate region of x, carrying all the light-front momenta of the nucleon.

Within this model for the case of the nucleon it was found [29,30] that the description of the peaking property of $xf_V(x)$ distribution requires a residual system to have a mass comparable with the pion mass. Thus the spectral function approach indirectly favored the existence of the structure in the nucleon resembling a pion cloud.

Another nontrivial observation within this approach was that at the starting $Q_0^2 = m_c^2$ (m_c is the mass of the charm quark) when one expects that the partonic picture to be relevant, the peaking position x_p of $xf_V(x)$ distribution satisfies an inequality $x_p \leqslant \frac{1}{4}$ (not $x_p = \frac{1}{3}$ as naively expected) independent to the parameters of the model. This inequality is confirmed by the modern phenomenological PDFs of nucleon. Overall, the model described reasonably well the valence PDFs of nucleons for the region $0.2 < x < 0.6$ underestimating at larger x which indicates the importance of hard mechanism in the generation of large x component of valence PDFs in the nucleon.

In the current work we extend the residual field approach for the description of pion valence PDFs. Our goal is to address following main questions by describing the peaking propery of $xf_V(x)$ distribution of pion: are there structure in the pion residual to $q\bar{q}$ valence quarks (like it was observed for the case of nucleon) and how much can the mean field distribution of the residual systemcontribute to the high x structure of pion PDFs? In this approach we introduce a new object, that is the light-front wave function of the residual system, whose parameters will be fixed by describing the the peak position and the height of the valence $xf_V(x)$ distribution. Once the parameters of this wave function is fixed its validity can be further verified by calculating other observables such as pion form-factors, generalized partonic and transverse momentum distributions as well as observables which enter in the target fragmentation of hadrons into pions in collider kinematics [31].

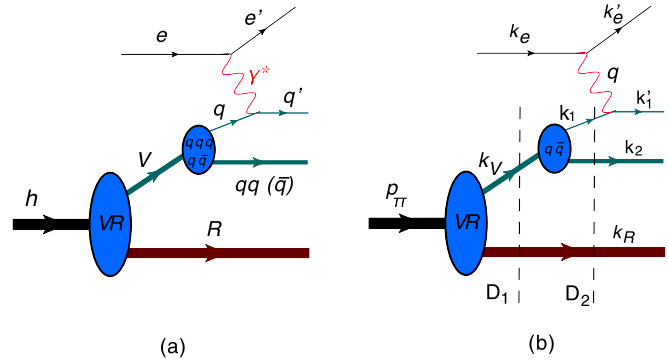


FIG. 1. Light-front diagrams for deep inelastic scattering in residual-mean field model. (a) General case for hadrons with qqq or $q\bar{q}$ valence clusters. (b) For the case of deep inelastic scattering from pion.

The outline for this work is as follows. Section II provides the description of the theoretical framework. In Section III we derive the PDFs based on the residual field model and in Sec. IV we introduce light-front wave function of two-body system, applying it for $q\bar{q}$-cluster and valence-residual systems, respectively. Section V presents numerical estimates of the model parameters following from the fit of the theoretical expression to the peak position and the height of $xf_V(x)$ distribution of the recently obtained empirical parametrization of pion PDFs [24,25]. Our focus in this comparison is to evaluate the relevant masses and the light-front momentum distribution of residual system. Furthermore using the obtained PDF at starting Q_0 we evolve it to the higher Q scale to compare our calcualtion with other empirical PDFs extracted from Drell-Yan experiment. Section VI contains conclusions and outlook for the further application of the presented approach in different processes.

II. THEORETICAL FRAMEWORK OF RESIDUAL FIELD MODEL

The residual field model utilizes conservation of valence parton quantum numbers to treat them as effective fermions whose numbers are conserved. It separates hadrons into a core of valence fermions consisting of massless quarks and a residual structure which contains everything besides the valence quarks, such as sea quarks and gluons. Interaction with the external probe in this case proceeds through the scattering off the valence quarks in the cluster. This picture is assumed to be valid for moderate to high $x \gtrsim 0.1$–0.2 and will break down at lower x, where the Regge dynamics dominate in the interaction.

According to the residual field model the deep inelastic scattering from a hadron in the leading approximation can be described by the light-front diagram of Fig.1(a) in which scattering takes place with a quark inside the valence cluster. The consideration of the residual system in the scattering amplitude is equivalent to the spectral function representation of the partonic structure of the hadron in which case the valence quark distribution is indirectly related to the dynamical characteristics of the residual system.

In light-front (LF) quantization one probes quantum fields at fixed light-cone time, $x^+ = t + z$, which provides several simplifications in describing high energy processes [32]. The LF approach provides a framework to study hadrons in terms of their light-front wave functions (LFWFs), in which case a hadron in a ket state represented by $|h\rangle$ can be described through the expansion in terms of the LFWFs $[\psi_{i/h}(\{x_i, \mathbf{k}_i\}_i)]$ [32,33]:

$$|h\rangle = \sum_i \int [d\mu_i] \psi_{i/N}(\{x_j, \mathbf{k}_j\}_j)|i\rangle, \tag{1}$$

where the sum is over all Fock states $|i\rangle$ and $[d\mu_i]$ is the relevant integration measure. Color and spin degrees of freedom have been suppressed.

With above wave functions the PDF for a quark of flavor i, in hadron, h can be represented as the expectation value of the number operator in the hadronic state [34,35]:

$$f_i(x, Q^2) = \int \frac{d^2\mathbf{k}_\perp}{(2\pi)^2} \langle h(p) \mid b_i^\dagger(xp, \mathbf{k}_\perp) b_i(xp, \mathbf{k}_\perp) \mid h(p)\rangle, \tag{2}$$

where $b_i^\dagger$ and b_i are creation and annihilation operators of parton i.

Except for the situations of high Q^2 and $x \to 1$ in which case one expects minimal-Fock component to dominate in Eq. (2), the calculation of hadronic PDF's at moderate x will require LFWFs which are the solution of infinite set of coupled integral equations, containing the different number of quark or gluon constituents. Thus often in practical calculations LFWFs are modeled. The modeling of the valence LFWFs for the pion has been done in different approaches such as harmonic oscillator models [36], models relating equal-time wave function to the light-front wave functions [37], light-front consitutent quark models [38], the Nambu–Jona-Lasinio model [36] as well as model based on light front holography [39,40].

Our approach in this work is phenomenological, instead of taking an infinite Fock state expansion as in Eq. (1), we approximate the $|h\rangle$ state through the transition of $\pi \to VR$, where V is a valence $q\bar{q}$ core and R is a residual state that absorbs all higher order Fock states as well as possible configurations (such as null-mass components) that may couple with $q\bar{q}$ cluster. Furthermore, we define phenomenological wave functions in such a way that they represent the solution of the Weinberg type equation on the light-front for $q\bar{q}$-cluster state (V), as well as for cluster-residual (VR) effective two-body state. Such wave functions are inherently nonperturbative and need to be modeled based on the prominent features of the structure of hadrons.

III. THE PION IN THE RESIDUAL FIELD MODEL

A. General formalism of deep-inelastic scattering

To set up derivational framework for pion PDF we consider probing the pion through deep inelastic electron scattering ($e\pi \to eX$). Using the universality of PDFs the results of calculation can be compared with PDFs extracted for example from Drell-Yan processes in $\pi N \to l^+l^- + X$ reactions. This is a consequence of the definition of PDFs and validity of QCD factorization for these processes.

Within one-photon exchange approximation the scattering takes place with the virtual photon γ^* with four-momentum $q^\mu = k_e^\mu - k_e'^\mu$, where k_e^μ and $k_e'^\mu$ are the four momenta of the initial and scattered electrons, respectively.

The cross section for the DIS process can be expressed through the contraction of leptonic and hadronic tensors as follows:

$$\frac{d\sigma}{dQ^2 dx} = \frac{2\pi\alpha^2 y^2}{Q^6} m_\pi L_{\mu\nu} W_\pi^{\mu\nu}, \tag{3}$$

where $Q^2 = -q^\mu q_\mu$, $y = \frac{p_\pi \cdot q}{p_\pi \cdot k_e}$ and the unpolarized leptonic tensor is

$$L_{\mu\nu} = 4\left[\left(k_{e,\mu} - \frac{q_\mu}{2}\right)\left(k_{e,\nu} - \frac{q_\nu}{2}\right)\right] + Q^2\left[-g_{\mu\nu} - \frac{q_\mu q_\nu}{Q2}\right]. \tag{4}$$

The hadronic tensor, $W_\pi^{\mu\nu}$, in general can be defined through the inelastic hadronic current $J^\mu(p_X, s_X, p_\pi, s_\pi)$ in the form

$$W_\pi^{\mu\nu} = \frac{1}{4\pi m_\pi} \int \sum_X \sum_{s_x} (J^\mu)^\dagger \times (p_X, s_X, p_\pi, s_\pi) J^\nu(p_X, s_X, p_\pi, s_\pi) \times (2\pi)^4 \delta^4(q + p_\pi - p_X) \delta\left(p_X^2 - M_x^2\right) \frac{d^4 p_x}{(2\pi)^3}. \tag{5}$$

In derivations, we will work with light-cone coordinates with the convention for four-momenta being

$$k^\mu = (k^+, k^-, \mathbf{k}^\perp) = (k^0 + k^3, k^0 - k^3, (k^1, k^2)). \tag{6}$$

The calculations are performed in the Drell-Yan-West reference frame where the four-momenta of the pion, p_π^μ, and virtual photon, q^μ are defined as follows:

$$p_\pi^\mu = \left(p_\pi^+, \frac{m_\pi^2}{p_\pi^+}, \mathbf{0}^\perp\right), \quad q^\mu = \left(0, \frac{2p_\pi \cdot q}{p_\pi^+}, \mathbf{q}^\perp\right), \tag{7}$$

where $q_\perp^2 = Q^2$.

In this reference frame the F_2 structure function of the pion is related to the $++$ component of the hadronic tensor as follows:

$$F_2(x, Q^2) = \frac{m_\pi Q^2}{2x(p_\pi^+)^2} W_\pi^{+,+} \tag{8}$$

and within the framework of QCD factorization and the definition of PDFs in leading order one can relate the PDF to the structure function F_2 as

$$F_2(x, Q^2) = \sum_i e_i^2 x f_i(x, Q^2), \tag{9}$$

where $f_i(x)$ was defined in Eq. (2) and i runs for quarks or antiquarks in the pion, interacting with the external probe. Comparing Eqs. (8) and (9) one observes that the calculation of PDFs is related to the calculation of the $++$ component of the hadronic tensor, $W_\pi^{\mu\nu}$.

In the case of valence quarks using the above relations allows us to extract sum of quark and anti-quark valence quark distributions weighted by x. Usually, invoking isospin symmetry it is assumed that the up valence distribution in π^+ is equal to the down valence distribution in π^-: $f_V(x,Q^2) = u_V^{\pi^+}(x,Q^2) = d_V^{\pi^-}(x,Q^2)$.

B. Hadronic current and hadronic tensor

For calculation of pion structure function we consider the diagram of Fig. 1(b) in which it is assumed that the pion transitions to the cluster of valence $q\bar{q}$ state and the residual state, R before the interaction of virtual photon with one of the valence quarks in the cluster takes place.

Identifying the hadronic current J^μ in Eq. (5) with the scattering amplitude A^μ, which corresponds to the part of the diagram of Fig. 1(b) without electron lines and virtual photon propagator and taking into account the phase space of final state quarks and residual system one obtains for the hadronic tensor

$$W^{\mu\nu}(x,Q^2) = \frac{1}{4\pi m_\pi}\sum_{\{h_i,\tau_i\}}\int \delta\left(k_R^2 - m_R^2\right) \times \frac{d^4k_R}{(2\pi)^3}\delta\left(k_1'^2 - m^2\right)\frac{d^4k_1'}{(2\pi)^3}\delta\left(k_2^2 - m^2\right)\frac{d^4k_2}{(2\pi)^3} \times (2\pi)^4\delta^{(4)}(p_\pi + q - \sum_{i=1}^{2} k_i - k_R)A^{\mu\dagger}A^\nu, \tag{10}$$

where the sum $\sum_{\{h_i,\tau_i\}}$ is over all the spins of the valence quarks and the residual system. The Lorentz invariant phase space evaluated in light-cone coordinates is

$$\delta(k^2 - m^2)d^4k = \frac{1}{2}\delta(k^+k^- - k_\perp^2 - m^2)dk^-dk^+d^2\mathbf{k}_\perp = \frac{dk^+d^2\mathbf{k}_\perp}{2k^+}|_{k^- = \frac{k_\perp^2+m^2}{k^+}} = \frac{dxd^2\mathbf{k}_\perp}{2x}|_{k^- = \frac{k_\perp^2+m^2}{xP_\pi^+}}, \tag{11}$$

where $x = \frac{k^+}{P_\pi^+}$ is the light-front momentum fraction of pion constituent with momentum k^+. For energy-momentum conservation one obtains

$$\delta^{(4)}(p_\pi + q - k_1' - k_2 - k_R) = 2\delta(p_\pi^+ + q^+ - k_1'^+ - k_2^+ - k_R^+) \times \delta(p_\pi^- + q^- - k_1'^- - k_2^- - -k_R^-) \times \delta^{(2)}(\mathbf{p}_\pi^\perp + \mathbf{q}^\perp - \mathbf{k_1'}^\perp - \mathbf{k_2}^\perp - \mathbf{k}_R^\perp). \tag{12}$$

Taking into account our choice of the reference frame Eq. (7) according to which $q^+ = 0$ and $k_1'^+ = k_1^+$ one obtains

$$\delta(p_\pi^+ + q^+ - k_1'^+ - k_2^+ - k_R^+) = \frac{1}{p_\pi^+}\delta(1 - x_1 - x_2 - x_R), \tag{13}$$

where $x_1 = \frac{k_1^+}{p_\pi^+}$, $x_2 = \frac{k_2^+}{p_\pi^+}$, and $x_R = \frac{k_R^+}{p_\pi^+}$. Using $k_1' = p_\pi - k_2 - k_3 - k_R$ and neglecting initial transverse momenta of pion constituent, compared to $q_\perp$, i.e., $k_{1,\perp}'^2 = (\mathbf{k}_{1,\perp} + \mathbf{q}_\perp)^2 \approx \mathbf{q}_\perp^2 \gg k_{1,\perp}^2$, as well as using the condition $p_\pi^+ \gg m_\pi, m_V, m_R, k_{1,2}^\perp, k_R$ one evaluates

$$\begin{aligned}\delta(p_\pi^- + q^- - k_1'^- - k_2^- - k_R^-) &= \delta\left(\frac{m_\pi^2}{p_\pi^+} + \frac{2p_\pi\cdot q}{p_\pi^+} - \frac{k_{1,\perp}'^2 + m^2}{x_1p_\pi^+} - \frac{k_{2,\perp}^2 + m^2}{x_2p_\pi^+} - \frac{k_{R,\perp}^2 + m_R^2}{x_Rp_\pi^+}\right)\\ &\approx \delta\left(\frac{2p_\pi\cdot q}{p_\pi^+} - \frac{Q^2}{x_1p_\pi^+}\right) = \frac{x_1p_\pi^+}{2p_\pi\cdot q}\delta(x_1 - x_B),\end{aligned} \tag{14}$$

where Bjorken x_B is defined as $x_B = \frac{Q^2}{2p_\pi\cdot q}$. Finally with the same conditions

$$\delta^{(2)}\left(\mathbf{p}_\pi^\perp + \mathbf{q}^\perp - \mathbf{k_1'}^\perp - \mathbf{k_2}^\perp - \mathbf{k}_R^\perp\right) = \delta^{(2)}\left(\mathbf{k_1}^\perp + \mathbf{k_2}^\perp + \mathbf{k}_R^\perp\right). \tag{15}$$

Using Eqs. (13)–(15) in Eq. (12) for hadronic tensor in Eq. (10) one arrives at

$$W^{\mu\nu}(x,Q^2) = \frac{1}{4m_\pi}\sum_{\{h_i,\tau_i\}}\int [dx][d^2\mathbf{k}_\perp]\frac{2x_1x_B}{Q^2}\delta(x_1 - x_B), \times A^{\mu\dagger}A^\nu, \tag{16}$$

where

$$[dx] = \delta(1 - x_1 - x_2 - x_R)\frac{dx_R}{x_R}\prod_{i=1}^{2}\frac{dx_i}{x_i}, [d^2\mathbf{k}_\perp] = 16\pi^3\delta^{(2)}\left(\sum_{i=1}^{2}\mathbf{k}_{i,\perp} + \mathbf{k}_{R,\perp}\right)\frac{d^2\mathbf{k}_{R,\perp}}{16\pi^3}\prod_{i=1}^{2}\frac{d^2\mathbf{k}_{i,\perp}}{16\pi^3}. \tag{17}$$

As it follows from Eqs. (8) and (9) to calculate the pion PDF one needs to evaluate the "+" component of the scattering amplitude A^μ.

C. Scattering amplitude in residual field model

To calculate the amplitude presented in Fig. 1(b) we use light-front diagrammatic rules [41]. Since momentum transferred to the quark/anti-quark in the pion is significantly larger than their initial momenta, the interference terms will be small and the cross section will represent the incoherent sum of the square of amplitudes corresponding to the scattering from quark and antiquark. Thus we first calculate amplitude of scattering from quark and then use the result to evaluate the scattering from the antiquark.

To calculate the amplitude we notice that the diagram of Fig. 1(b) is characterized by two intermediate states (indicated by vertical dashed lines) that are defined by two light-front propagators. With the momenta assigned for each particles in

the scattering defined in the diagram one obtains

$$A^{\mu}(k_1', h_1', k_2, h_2, k_R, h_R) = \sum_{h_V} \frac{\bar{u}(k_1', h_1') i e_q \gamma^{\mu} (\not{k}_1 + m_q) v(k_2, h_2) \Gamma^{V\to q\bar{q}} \chi_V}{k_1^+ D_2} \times \frac{\chi_V^{\dagger} \chi_R^{\dagger} \Gamma^{\pi\to VR} \chi_{\pi}}{k_V^+ D_1}, \tag{18}$$

where $\Gamma^{\pi\to VR}$ is the effective vertex for the transition of pion into valence $q\bar{q}$ cluster V and a residual state R, and the $\Gamma^{V\to q\bar{q}}$ vertex describes the transition of the cluster, V to the valence quark and antiquark. Also, h_i and h_1' are the helicities of the ith valence quark before and after the interaction with virtual photon.

For the denominators D_1 and D_2 according to light-front diagrammatic rules, one has

$$D_1 = p_{\pi}^- - k_R^- - k_V^- = \frac{1}{p_{\pi}^+}\left(m_{\pi}^2 - \frac{k_{R\perp}^2 + m_R^2}{x_R} - \frac{k_{V\perp}^2 + m_V^2}{x_V}\right) \tag{19}$$

and

$$D_2 = p_V^- - k_1^- - k_2^- - = \frac{1}{k_V^+}\left(m_V^2 - \frac{k_{1\perp}^2 + m^2}{\beta_1} - \frac{k_{2\perp}^2 + m^2}{\beta_2}\right), \tag{20}$$

where $\beta_i = \frac{x_i}{x_V}$ for $i = 1, 2$ quark and antiquark.

Furthermore, we use LF sum rule for the numerator of the propagator of off-shell quark with momentum k_1 [41]:

$$(\not{k}_1 + m) = \sum_{h_1} u(k_1, h_1)\bar{u}(k_1, h_1) + \frac{\gamma^+ (k_1^2 - m^2)}{k_1^+}, \tag{21}$$

and notice that since we are interested in the + component of the scattering amplitude, A^{μ}, and due to the relation $\gamma^+\gamma^+ = 0$, the second part of Eq. (21) does not contribute to the + component of the amplitude. Inserting the first part of Eq. (21) into Eq. (18) one introduces a phenomenological LF wave function for the valence-residual system

$$\psi_{VR}(x_V, \mathbf{k}_{R,\perp}, x_R, \mathbf{k}_{V,\perp}) = \frac{\bar{\chi}_V \bar{\chi}_R \Gamma^{\pi\to VR}}{m_{\pi}^2 - \frac{k_{V,\perp}^2 + m_V^2}{x_V} - \frac{k_{R,\perp}^2 + m_R^2}{x_R}} \tag{22}$$

and similarly for the $q\bar{q}$ cluster

$$\psi_{q\bar{q}}(\beta_1, \beta_2, \mathbf{k}_{1,\perp}, \mathbf{k}_{2,\perp}) = \frac{\bar{u}(k_1, h_1)\Gamma^{V\to q\bar{q}} v(k_2, h_2)\chi_V}{m_V^2 - \sum_{i=1}^{2} \frac{k_{i,\perp}^2 + m_i^2}{\beta_i}}, \tag{23}$$

where χ_V and χ_R represent the helicity wave functions for the cluster and residual system, respectively.

In further derivation we assume that the residual state has a zero helicity and the quantum number of $q\bar{q}$ cluster is defined by the quantum number of the pion. Writing then the helicity wave function of the cluster explicitly: $\xi_{q\bar{q}} = \frac{u(k_1,h_1)\bar{v}(k_2,-h_1) - u(k_1,-h_1)\bar{v}(k_2,h_1)}{\sqrt{2}}$, for the "+" component of the scattering amplitude one obtains

$$A^{+}(k_1', h_1', k_2, -h_1, k_R) = \left[\bar{u}(k_1', h_1') i e_q \gamma^{+} u(k_1, h_1) \frac{\psi_{q\bar{q}}(\beta_1, \beta_2, \mathbf{k}_{1,\perp}, \mathbf{k}_{2,\perp})}{\sqrt{2}\beta_1} - \bar{v}(k_1, h_1) i e_{\bar{q}} \gamma^{+} v(k_1', h_1') \frac{\psi_{q\bar{q}}(\beta_1, \beta_2, \mathbf{k}_{1,\perp}, \mathbf{k}_{2,\perp})}{\sqrt{2}\beta_1}\right] \times \frac{\psi_{VR}(x_V, \mathbf{k}_{R,\perp}, x_R, \mathbf{k}_{V,\perp})}{x_V}. \tag{24}$$

By neglecting the masses of valence quarks, one evaluates only helicity conserving term of the matrix elements of $\bar{u}(k_1', h_1')\gamma^{+} u(k_1, h_1) = \bar{v}(k_1, h_1)\gamma^{+} v(k_1', h_1') = 2k_1^{+}\delta^{h_1', h_1}$. This results in

$$A^{+}(k_1', h_1, k_2, -h_1, k_R) = \left[2k_1^{+} i e_q \frac{\psi_{q\bar{q}}(\beta_1, \beta_2, \mathbf{k}_{1,\perp}, \mathbf{k}_{2,\perp})}{\sqrt{2}\beta_1} - 2k_1^{+} i e_{\bar{q}} \psi_{q\bar{q}}(\beta_1, \beta_2, \mathbf{k}_{1,\perp}, \mathbf{k}_{2,\perp}) \times \frac{}{\sqrt{2}\beta_1}\right] \frac{\psi_{VR}(x_V, \mathbf{k}_{R,\perp}, x_R, \mathbf{k}_{V,\perp})}{x_V}. \tag{25}$$

D. Valence parton distribution

Inserting Eq. (25) into the expression of the hadronic tensor in Eq. (16), summing by helicites of final quarks and using relations of Eqs. (8) and (9) for the valence quark distribution one obtains

$$f_V(x_B, Q^2) = \int \frac{dx_1 d^2\mathbf{k}_{1,\perp}}{16\pi^3 x_1} \frac{dx_2 d^2\mathbf{k}_{2,\perp}}{16\pi^3 x_2} \frac{dx_R d^2\mathbf{k}_{R,\perp}}{16\pi^3 x_R} \times \delta(x_1 - x_B) 16\pi^3 \delta(1 - x_1 - x_2 - x_R) \times \delta^{(2)}\left(\sum_{i=1,2,R} \mathbf{k}_{i,\perp}\right) | \Psi_{q\bar{q}}(\beta_1, k_{1,\perp}, \beta_2, k_{2,\perp}) \times |^2 | \Psi_{VR}(x_R, k_{R,\perp}) |^2 . \tag{26}$$

Expecting that light-front wave function of the $q\bar{q}$ system will depend on relative transverse momentum and relative light-front momentum fractions only, we can factorize above integrals by introducing transverse momentum of quark and antiquark in the center of mass of the $q\bar{q}$ system:

$$\tilde{\mathbf{k}}_{i,\perp} = \mathbf{k}_{i,\perp} - \beta_i \mathbf{k}_{V,\perp} \quad \text{(i=1,2)}. \tag{27}$$

Substituting Eq. (27) into Eq. (26), one can factorize the integration by $k_{R,\perp}$. Furthermore integrating over x_2 results in

$$f_V(x_B, Q^2) = \int_0^{1-x_B} \frac{dx_R}{(16\pi^3)^2 x_B (1 - x_B - x_R) x_R} \times \left[\int^{Q^2} d^2\tilde{\mathbf{k}}_{1,\perp} d^2\tilde{\mathbf{k}}_{2,\perp} \delta^2(\tilde{\mathbf{k}}_{1,\perp} + \tilde{\mathbf{k}}_{2,\perp}) \times |\Psi_{q\bar{q}}(\beta_1, \tilde{\mathbf{k}}_{1,\perp})|^2 \int^{Q^2} d^2\mathbf{k}_{R,\perp} \times |\psi_{VR}(x_R, \mathbf{k}_{R,\perp})|^2\right]. \tag{28}$$

The above expression can be integrated by $d^2\tilde{k}_{2,\perp}$ using the $\delta^2()$ function and renaming $\beta_1 \equiv \beta$ and $k_{1,\perp} \equiv k_\perp$ one obtains

$$f_V(x_B, Q^2) = \int_0^{1-x_B} \frac{dx_R}{(16\pi^3)^2 x_B(1-x_B-x_R)x_R} \times \left[\int^{Q^2} d^2\mathbf{k}_\perp |\Psi_{q\bar{q}}(\beta, \mathbf{k}_\perp)|^2\right]_{q\bar{q}} \times \left[\int^{Q^2} d^2\mathbf{k}_{R,\perp} |\psi_{VR}(x_R, \mathbf{k}_{R,\perp})|^2\right]_{VR}, \quad (29)$$

where $[\cdots]_{q\bar{q}}$ and $[\cdots]_{VR}$ we can interpret as response functions of the $q\bar{q}$ valence-cluster and residual systems, respectively.

IV. MODELING NONPERTURBATIVE LIGHT-FRONT WAVE FUNCTIONS

A. General approach for two-body relativistic LFWF

To model $q\bar{q}$ cluster and VR wave functions we first note that both are two-body wave functions for which relativistic normalization is defined as follows:

$$\int |\Psi^{LF}(k_{12})|^2 \frac{dy}{y(1-y)} \frac{d^2k_{12,\perp}}{16\pi^3} = N, \quad (30)$$

where

$$y = \frac{k_1^+}{p_T^+} \quad (31)$$

with k_1^μ and p_T^μ being four-momenta of one of the bound particles and the target. Here, the relative momentum in the c.m. frame of two particle system is

$$k_{12}^2 = \frac{(s_{12}-(m_1-m_2)^2)(s_{12}-(m_1+m_2)^2)}{4s_{12}} = \frac{m_1^2(1-y)+m_2^2 y + k_{12,\perp}^2}{4y(1-y)} - \frac{m_1^2+m_2^2}{2} + \frac{\left(m_1^2-m_2^2\right)^2 y(1-y)}{4\left(m_1^2(1-y)+m_2^2 y + k_{12\perp}^2\right)} \quad (32)$$

and

$$s_{12} = \frac{m_1^2(1-y)+m_2^2 y + k_{12,\perp}^2}{y(1-y)}. \quad (33)$$

We model LF wave function similar to [42,43] assuming factorization of the relative momentum wave function in the c.m. system and the absence of inelastic transitions in two-body wave function. This allows to relate the c.m. wave function to the nonrelativistic wave function evaluated at the relative momentum defined relativistically in Eq. (32):

$$\Psi_{12}^{LF}(k_{12}) = \Psi_{12}^{NR}(k_{12}) \sqrt{\frac{E_1 E_2}{E_1+E_2} 16\pi^3}. \quad (34)$$

Here, nonrelativistic wave function is normalized as follows:

$$\int |\Psi^{NR}(k_{12})|^2 d^3k_{12} = N. \quad (35)$$

It is worth noting that due to relativistic normalization in Eq. (30) and definition of the light-front relative momentum k_{12} in Eq. (32), the $k_{12} \to \infty$ corresponds to the limits of $y \to 0, 1$, thus excluding nonphysical region of momenta entering in the argument of LF wave function (as it is the case of nonrelativistic wave functions).

The normalization factor N, in Eqs. (30) and (35) in general should be fixed through observables, such as baryonic number (or number of constituents) [44,45], or form factor of the system [46], etc. For example, for the case of baryons the valence quark wave function's normalization can be fixed by the baryonic number [30]. However, a situation with pion introduces some uncertainty since the baryonic number is zero and this issue will be discussed below.

1. Soft $q\bar{q}$ wave function

Assuming quark masses are the same, the above approach can be used to model the soft $q\bar{q}$ wave function in the form

$$\Psi_{q\bar{q}}^{LF}(\beta, k_{12,\perp}) = \sqrt{8\pi^3 E_k}\, \Psi_{q\bar{q}}^{NR}(k_{12}), \quad (36)$$

where $E_k = \sqrt{m^2+k_{12}^2}$ and $\vec{k}_{12} = (k_{12,z}, \vec{k}_{12,\perp})$ is the relative momentum in the $q\bar{q}$ c.m. system with the magnitude

$$k_{12} = \sqrt{\frac{m^2+k_{12,\perp}^2}{4\beta(1-\beta)} - m^2}. \quad (37)$$

We normalize the $q\bar{q}$ wave function per one quark (or antiquark) in the cluster since in the calculation of the PDF we sum by individual contributions of valence quarks. We also take into account that the normalization is less than unity since no hard component is included in the cluster wave function which can be generated through the hard gluon exchanges [41]. With this, the normalizetion is fixed as

$$\int |\Psi^{LF} q\bar{q}(k_{12})|^2 \frac{d\beta}{\beta(1-\beta)} \frac{d^2k_{12,\perp}}{16\pi^3} = N_{q\bar{q}} = 1-h. \quad (38)$$

Note that in addition to the hard component the parameter h also accounts for the fact that at $x < 0.1$, the Regge dynamics may play a role in PDF which is not included in the current calculations.

For nonrelativistic wave function we use a harmonic oscillator type wave function with free parameters, A_V and B_V:

$$\Psi_{q\bar{q}}^{NR}(k) = A_V \exp\left[-\frac{B_V}{2}k_{12}^2\right]. \quad (39)$$

A number of previous works have used the similar wave functions or a form similar to it [28,39,41,47,48]. Using the above light-front wave function, Eq. (36), for the $q\bar{q}$ system's

response function defined in Eq. (29), one obtains

$$\left[\int^{Q^2} d^2\mathbf{k}_\perp |\Psi_{q\bar{q}}(\beta,\mathbf{k}_\perp)|^2\right]_{q\bar{q}} = 8\pi^3 \int^{Q^2} d^2k_\perp E_k A_V^2 e^{-B_V \frac{k_\perp^2}{4\beta(1-\beta)}} = 8\pi^3 \int^{Q^2} d^2\mathbf{k}_\perp \sqrt{\frac{k_\perp^2}{4\beta(1-\beta)}} e^{-B_V \frac{k_\perp^2}{4\beta(1-\beta)}} = \frac{16\pi^4\sqrt{\pi}A_V^2}{B_V^{\frac{3}{2}}}\beta(1-\beta) = 16\pi^3 N_{q\bar{q}}\beta(1-\beta). \quad (40)$$

Here, in the last step we neglected by the masses of the valence quarks and assumed $Q^2 \gg k_\perp^2$ (consistent with collinear approximation). This allowed to calculate the integral analytically, in which we set the upper limit of the integration to ∞. It is interesting that in the massless limit because of the relation of Eq. (37) the integral in the right-hand side part of the equation has an analytic form of the normalization of the NR wave function in the center of mass of $q\bar{q}$ system. As a result the response function depends on the overall normalization factor $N_{q\bar{q}} = \frac{\pi^{\frac{3}{2}}A_V^2}{B_V^{\frac{3}{2}}}$ while momentum distribution, $\beta(1-\beta)$, is similar to the one obtained from perturbative wave function.

It is worth mentioning that the calculated in this way $q\bar{q}'$s response function peaks at $\beta = \frac{1}{2}$ which is consistent with relativistic wave function of massless $q\bar{q}$ system.

2. *Light-front wave function of valence-residual system*

To calculate the response function of residual system one has to model the light-front wave function of valence-residual system. Here, we use a harmonic oscillator (HO) type wave function in Eq. (34) obtaining

$$\Psi_R^{LF}(x_R, k_{R,\perp}) = A_R\sqrt{16\pi^3}\sqrt{\frac{E_V E_R}{E_V+E_R}} e^{-\frac{B_R}{2}k_R^2}, \quad (41)$$

where $E_V = \sqrt{m_V^2 + k_R^2}$, $E_R = \sqrt{m_R^2 + k_R^2}$. The k_R is the three-dimensional momentum defined in the center of mass of the $V-R$ system:

$$k_R^2 = \frac{(s_{VR} - (m_V - m_R)^2)(s_{VR} - (m_V + m_R)^2)}{4s_{VR}}, \quad (42)$$

where

$$s_{VR} = \frac{k_{R,\perp}^2 + m_R^2}{x_R} + \frac{k_{R,\perp}^2 + m_V^2}{1-x_R} \quad (43)$$

resulting in

$$k_R^2 = \frac{m_R^2(1-x_R) + m_V^2 x_R + k_{R,\perp}^2}{4x_R(1-x_R)} - \frac{m_R^2 + m_V^2}{2} + \frac{\left(m_R^2 - m_V^2\right)^2 x_R(1-x_R)}{4\left(m_R^2(1-x_R) + m_V^2 x_R + k_{R\perp}^2\right)}. \quad (44)$$

The above defined wave function is normalized as follows:

$$\int |\Psi_R^{LF}(k_{12})|^2 \frac{dy}{x_R(1-x_R)} \frac{d^2k_{R,\perp}}{16\pi^3} = N_R, \quad (45)$$

where the normalization, N_R, one can interpret as the number of constituents in the residual hadronic system.

Using the above expressions for the VR wave function and the relative momentum k_R [Eq. (42)], for the response function of the VR system, one obtains the following:

$$R(x_R) = \left[\int^{Q^2} d^2\mathbf{k}_{R,\perp} |\psi_{VR}(x_R, \mathbf{k}_{R,\perp})|^2\right]_{VR} = 16\pi^3 A_R^2 \int^{Q^2} d^2\mathbf{k}_{R,\perp} \frac{E_V E_R}{(E_V+E_R)} e^{-B_R k_R^2}. \quad (46)$$

Note that in the above equation masses of the valence cluster m_V, and residual state m_R, are virtual and characterize the transition into nonstationary virtual state of a valence cluster and the residual system, thus they do not need to correspond to the pion mass.

B. Modeled soft pion PDF

Inserting Eqs. (40) and (46) into Eq. (29) and using normalization condition of Eq. (38), for the modeled parton distribution of pion one obtains

$$f_V(x_B, Q^2) = N_{q\bar{q}} A_R^2 \int_0^{1-x_B} \frac{dx_R}{x_R} \frac{1}{(1-x_R)^2} \times \left[\int^{Q^2} d^2\mathbf{k}_{R,\perp} \frac{E_V E_R}{(E_V+E_R)} e^{-B_R k_R^2}\right]. \quad (47)$$

The obtained expression indicates that, the $\beta(1-\beta)$-relative light-cone momentum fraction distribution of valence quarks in the cluster [Eq. (40)] results in an only x_R dependent integrand in Eq. (47), convoluted with the response function of the residual system [Eq. (46)]. In the current model this follows from the neglecting the valence quark masses. As Eq. (47) shows the shape of the PDF depends on the slope factor of the cluster-residual system's momentum distribution, B_R, as well as the respective virtual masses of the cluster m_V and the residual system m_R.

V. NUMERICAL RESULTS

A. Parameters of the model

We use recent results from the JAM collaboration [24,25] on pion PDF to fit Eq. (47).

Our main focus in the fitting procedure is to describe the position and the height of the x weighted parton distribution in accordance with our model's assumption that these features of valence PDFs are characterized by the soft partonic dynamics. We expect that perturbative processes such as hard gluon exchanges [26–28] between valence quarks to contribute to the $x \to 1$ part of the PDF and as such it is out of domain of the current model.

As follows from Eq. (47) the masses of residual (m_R) and valence (m_V) systems, as well as the width of the VR

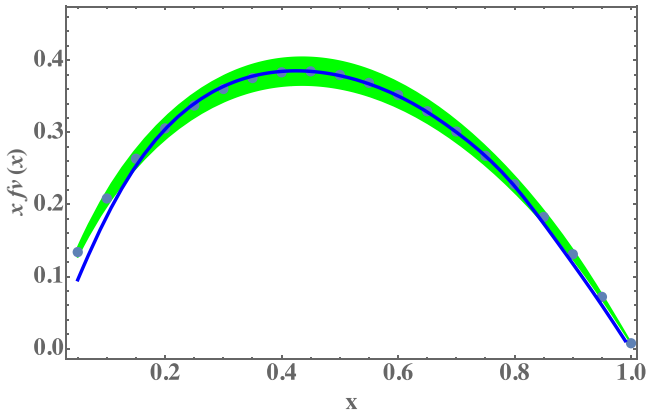


FIG. 2. Description of x-weighted pion PDF at $Q_0 = 1.3$ GeV for $m_R = 0$, $m_V = 0.95$ GeV, and $B_R = 1.2$ GeV^{-2}.

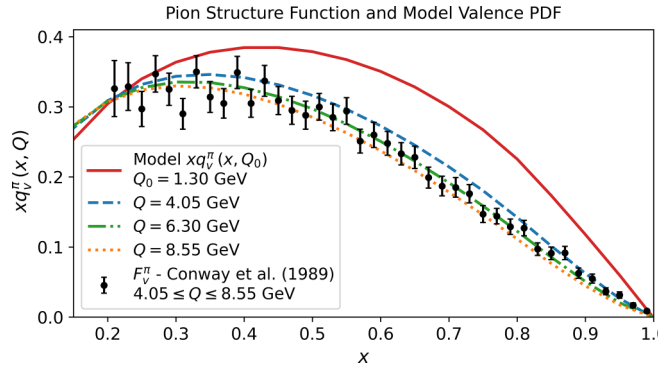


FIG. 3. Model pion PDF evolved to different Q^2, compared to the experimentally extracted pion structure functions.

distribution, B_R, define the shape of the PDF that produces the peaking distribution of the PDF weighted by x.

We choose the starting $Q^2 = Q_0^2 = 1.69$ GeV^2, the scale Q_0, chosen in JAM parametrization to be the c-quark mass. The fitting analysis indicates that the position of the peak can be reproduced only if the virtual mass of the residual system is close to zero, $m_R \approx 0$. This is very different from our analysis of the nucleon PDF's within the same residual field model [29,49] in which we found that the residual mass for the best fit is close to the pion mass, $m_R^N \approx 0.14$, indicating the validity of meson cloud picture of valence parton distribution in the nucleon.

The best fit of the JAM pion PDF is presented in Fig. 2, for the parameters of $m_R = 0$, $m_V = 0.95$ GeV, and $B_V = 1.2\text{GeV}^{-2}$. Note that the qualitative agreement of the data requires $m_V \approx Q_0$ and $m_R \approx 0$. As the figure shows, the soft mechanism describes the empirical PDF reasonably well in the range of $0.1 < x < 0.85$. Even though our goal was not to describe the $x \to 1$ part of the pion PDF, it is interesting to observe that the considered residual field model describing the soft mechanism of interaction, predicts a considerable contribution to the high x part of the pion PDF leaving little room for the hard mechanism in the generation of PDF at large x.

B. Comparison with other extractions of pion PDFs

In general, the pion PDFs are extracted from two types of high energy processes: pion-induced Drell-Yan scatterings and semi-inclusive leading-neutron deep-inelastic reactions refereed to as Sullivan processes. The existing PDFs extracted from Sullivan processes are constrained in the small-x region, approximately $x \lesssim 0.05$ [21], which are dominated by sea quark and gluon PDFs having negligible contribution from valence quark dynamics. The valence quark region is probed in Drell-Yan processes [50–52] measured in high $m_{\mu\bar{\mu}} > 4$ GeV region.

To verify the consistency of our calculation with pion PDFs measured at higher Q^2, we compare our calculation with the PDFs extracted from Fermi-Lab Drell-Yan data [52] on $\pi^- N \to \mu^+\mu^- X$ scattering which are measured for dimuon mass range of $4.05 < Q < 8.55$ GeV with ($Q \approx m_{\mu\mu}$).

To compare with these PDFs we performed QCD evolution of our calculation at starting Q_0 to the Q values measured at Fermi Lab. The QCD evolution is performed by using, Evolution Kernel Operators (EKO) library [53], which solves the DGLAP evolution equations in Mellin space. The evolution was carried out at leading order with the one-loop coupling chosen to reproduce $\alpha_s(M_Z) = 0.1180$, the global central value from PDG [54]. For comparison we evolved our model pion valence distribution at at the initial scale, Q_0 to Q scales corresponding to lower, central, and upper portions of the Conway *et al.* [52] kinematic range

Figure 3 shows a comparison of evolved calculations for above mentioned Q scales with the extracted PDF data. We also present our model calculation for the initial scale, Q_0.

As seen in Fig. 3, the structure function computed from the PDFs of the evolved model agrees well with the experimental data. This agreement is consistent with the good agreement of our model with the pion PDF obtained by JAM collaboration at low Q scale [24,25].

It is worth noting that although PDFs are scheme- and scale-dependent theoretical quantities rather than physical observables, once the factorization scheme, scale, and perturbative order (LO in this work) are specified consistently, the scheme- and scale-dependent PDFs provide a well-defined prediction for measurable structure functions.

C. Interpretation of the results

The parameters of the model that provide the best fit to the empirical PDF (Fig. 2) allow to ascertain the mechanism dominating parton dynamics at the x range where the peak of the x-weighted PDF distribution is observed. For this, we first analyze the response function of the residual system presented in Eq. (46). As Fig. 4 shows the response function at starting Q_0, has a wide distribution in x_R, slightly peaking at $x_R \approx 0.5$. The distribution of the response function saturates at higher Q^2 with the peaking at $x_R = 0.5$ becoming more pronounced. This indicates that the valence $q\bar{q}$ system as a whole carries a total momentum fraction $x_V = 1 - x_R \approx 0.5$.

Since x Bjorken corresponds to the light-front momentum fraction of the interacting quark with the relation

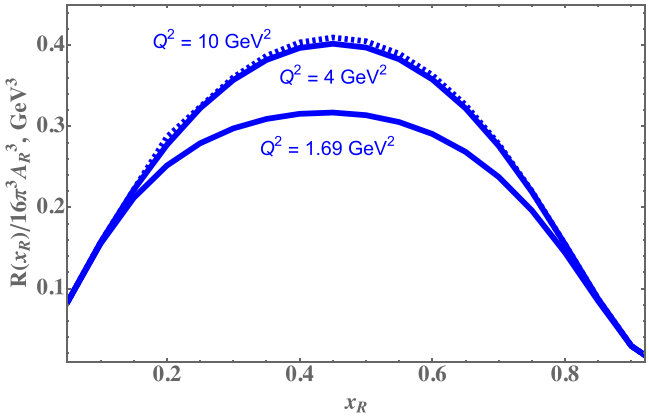


FIG. 4. The x_R dependence of response function $R(x_R)$ at different Q^2.

$x \approx \beta(1 - x_R)$, where β is the LF momentum fraction of the $q\bar{q}$ cluster carried by the interacting quark, and since the broad distribution of x_R, one observes that for $x \gtrsim 0.5$, relative momentum fraction, $\beta \approx 1$. This indicates that the observed distribution favors the dominance of the Feynman mechanism [55] according to which the interacting quark carries the most of the light-front momentum fraction of the cluster, with remaining LF momenta distributed among the wee partons in the residual system.

Another observation (as noted above) is the result of $m_R \approx 0$. This indicates that the residual system does not exhibit any structure (as it was the case for valence PDFs of nucleons [30]). On the other hand, the large value of $m_V \approx 0.95$ GeV indicates the large virtuality of the interacting quark comparable to Q_0 of the probe. This together with the relatively large B_R indicates that while interacting valence quark is highly virtual, the residual system is spread over the bulk size of the pion. This picture is consistent with the phenomenology that nucleon-nucleon interactions at large distances ($\geqslant 1.5$ fm) proceeds through the pion exchange in which no quark-interchanges are involved.

The overall constant in Eq. (47) is evaluated at $\sqrt{N_{q\bar{q}}}A_R = \sqrt{1-h}A_R \approx 0.86$. Assuming that overall Regge and high momentum mechanism contribute to $h \approx 0.2$, one obtains for the normalization of the residual LF wave function in Eq. (45) $N_R \approx 4$. This will predict, for example, that integrated multiplicity for pion in the target fragmentation region to be above 2.

Finally, the surprising result of the fit is that the considered model leaves little room for hard mechanism of high x PDF generated through the hard gluon exchange between valence $q\bar{q}$ system. The current result favors a pion structure dominated by soft mechanism of valence quark interaction. Moreover, it is interesting that $f_V(x) \mid_{x\to 1} \approx (1-x)$ consistent with the $f_V(x) \approx 1 - x$ distribution at the intermediate region in which case $x f_V(x) \approx x(1-x)$ peaks at $x_p \approx 0.5$ in agreement with the data. The latter reinforces the observation that high x structure of pion PDF has large soft component that defines also the peaking properties of $x f_V(x)$ distribution.

VI. CONCLUSION AND OUTLOOK

We have calculated pion valence parton distribution within residual field model, which was previously applied to the calculation of nucleon PDFs. Our focus is the intermediate region of x where the x weighted PDF has peaking property.

The model assumes no hard interaction between valence quarks in the cluster and it separates $q\bar{q}$ valence cluster (V) from the residual system (R). Both $q\bar{q}$ and VR systems are described by nonperturbative light-front wave functions that satisfies relativistic normalization. These wave functions allow to introduce the residual response function as well as the response function of the $q\bar{q}$ valence cluster. The pion PDF represents the convolution of these response functions. We analyzed the parameters of the model by fitting the position and the height of the x-weighted PDF to the empirical JAM18 distribution.

The fitting indicates that one can describe the above attributes of pion PDF only if the mass of the residual system is close to zero. However, we obtain large virtual mass for the $q\bar{q}$ cluster comparable to the Q_0 of the probe. Analysis of the response function of the residual system indicates that the dominant mechanism is similar to the Feynman mechanism in which interacting parton carries almost all the momentum of the valence quark system, with the remaining light-front momentum distributed to the noninteracting wee partons.

The fit allows to describe the empirical PDF reasonably well in the range of $0.1 \leqslant x \leqslant 0.85$ leaving little room for the hard mechanism of generating PDFs at large x. Even though our calculation underestimates the empirical PDF at $x \geqslant 0.85$, its substantial contribution in this region indicates that the inclusion of the hard gluon exchange mechanism in generation of parton PDFs at $x \to 1$ will require the consideration of the interference between soft and hard amplitudes that can introduce the exponent, $\beta < 2$ in $(1-x)^\beta$ distribution at $x \to 1$. Note that the $\beta = 2$ prediction is based on the assumption of negligible contribution from the soft amplitude in the $x \to 1$ region (see, e.g., Ref. [28]).

Finally, with the parameters of light-front wave function of residual system fixed, one will be able to make numerical predictions for different observables such as electromagnetic form factors, generalized parton distribution functions (GPDs), or transverse momentum dependent parton distribution functions (TMDs) in pion. These will allow an additional verification of the model. Additionally, the modeled residual state wave function allows to evaluate the fragmentation of pion in the backward kinematic region that can be probed in the EIC collider kinematics.

ACKNOWLEDGMENT

This work is supported by United States Department of Energy grant under Contract No. DE-FG02-01ER41172.

DATA AVAILABILITY

There are no publicly available research data or software supporting this manuscript. Requests for further information or data should be sent to the authors.

[1] T. Shigetani, K. Suzuki, and H. Toki, Pion structure function in the Nambu and Jona-Lasinio model, Phys. Lett. B **308**, 383 (1993).

[2] A. V. Belitsky, Quark distribution in the pion from QCD sum rules with nonlocal condensates, Phys. Lett. B **386**, 359 (1996).

[3] B. L. Ioffe and A. G. Oganesian, Improved calculations of quark distributions in hadrons: The case of the pion, Eur. Phys. J. C **13**, 485 (2000).

[4] A. G. Oganesian, Quark distributions in QCD sum rules: Unexpected features and paradoxes, Phys. At. Nucl. **71**, 1439 (2008).

[5] S. J. Brodsky and C.-R. Ji, Applications of quantum chromodynamics to hadronic and nuclear interactions, Lect. Notes Phys. **248**, 153 (1986).

[6] T. Frederico and G. A. Miller, Deep-inelastic structure function of the pion in the null-plane phenomenology, Phys. Rev. D **50**, 210 (1994).

[7] B. C. Tiburzi and G. A. Miller, Generalized parton distributions and double distributions for $q\bar{q}$ pions, Phys. Rev. D **67**, 113004 (2003).

[8] B. Pasquini, S. Rodini, and S. Venturini (MAP Collaboration), Valence quark, sea, and gluon content of the pion from the parton distribution functions and the electromagnetic form factor, Phys. Rev. D **107**, 114023 (2023).

[9] H.-M. Choi and C.-R. Ji, Consistency of the pion form factor and unpolarized transverse momentum dependent parton distributions beyond leading twist in the light-front quark model, Phys. Rev. D **110**, 014006 (2024).

[10] H. G. P, S. Puhan, A. K. P., R. Pandey, H. Dahiya, A. Kumar, and S. Dutt, Pion parton distribution functions in the light-cone quark model and experimental constraints, Phys. Rev. D **114**, 016010 (2026).

[11] S. J. Brodsky and G. F. de Téramond, Light-front dynamics and AdS/QCD correspondence: The pion form factor in the space- and time-like regions, Phys. Rev. D **77**, 056007 (2008).

[12] R. J. Holt and C. D. Roberts, Nucleon and pion distribution functions in the valence region, Rev. Mod. Phys. **82**, 2991 (2010).

[13] M. Ding, K. Raya, D. Binosi, L. Chang, C. D. Roberts, and S. M. Schmidt, Symmetry, symmetry breaking, and pion parton distributions, Phys. Rev. D **101**, 054014 (2020).

[14] X. Gao, L. Jin, C. Kallidonis, N. Karthik, S. Mukherjee, P. Petreczky, C. Shugert, S. Syritsyn, and Y. Zhao, Valence parton distribution of the pion from lattice QCD: Approaching the continuum limit, Phys. Rev. D **102**, 094513 (2020).

[15] J. Lan, C. Mondal, S. Jia, X. Zhao, and J. P. Vary, Pion and kaon parton distribution functions from basis light front quantization and QCD evolution, Phys. Rev. D **101**, 034024 (2020).

[16] M. Glück, E. Reya, and A. Vogt, Pionic parton distributions, Z. Phys. C - Particles and Fields **53**, 651 (1992).

[17] P. J. Sutton, A. D. Martin, R. G. Roberts, and W. J. Stirling, Parton distributions for the pion extracted from Drell-Yan and prompt photon experiments, Phys. Rev. D **45**, 2349 (1992).

[18] M. Glück, E. Reya, and I. Schienbein, Pionic parton distributions revisited, Eur. Phys. J. C **10**, 313 (1999).

[19] K. Wijesooriya, P. E. Reimer, and R. J. Holt, Pion parton distribution function in the valence region, Phys. Rev. C **72**, 065203 (2005).

[20] M. Aicher, A. Schäfer, and W. Vogelsang, Soft-gluon resummation and the valence parton distribution function of the pion, Phys. Rev. Lett. **105**, 252003 (2010).

[21] S. Chekanov, D. Krakauer, S. Magill, B. Musgrave, A. Pellegrino, J. Repond, R. Yoshida, M. C. K Mattingly, P. Antonioli, G. Bari, M. Basile, L. Bellagamba, D. Boscherini, A. Bruni, G. Bruni, G. CaraRomeo, L. Cifarelli, F. Cindolo, A. Contin, M. Corradi, *et al.* (ZEUS Collaboration), Leading neutron production in e^+p collisions at HERA, Nucl. Phys. B **637**, 3 (2002).

[22] A. Accardi, M. E. Christy, C. E. Keppel, P. Monaghan, W. Melnitchouk, J. G. Morfin, and J. F. Owens, New parton distributions from large-x and low-Q^2 data, Phys. Rev. D **81**, 034016 (2010).

[23] F. D. Aaron, C. Alexa, V. Andreev, B. Antunovic, S. Backovic, A. Baghdasaryan, E. Barrelet, W. Bartel, K. Begzsuren, A. Belousov, J. C. Bizot, V. Boudry, I. Bozovic-Jelisavcic, J. Bracinik, G. Brandt, M. Brinkmann, V. Brisson, D. Bruncko, A. Bunyatyan, G. Buschhorn, *et al.* (H1 Collaboration) Measurement of leading neutron production indeep-inelasticscattering at HERA, Eur. Phys. J. C **68**, 381 (2010).

[24] P. C. Barry, N. Sato, W. Melnitchouk, and C.-R. Ji, First Monte Carlo global QCD analysis of pion parton distributions, Phys. Rev. Lett. **121**, 152001 (2018).

[25] P. C. Barry, C.-R. Ji, N. Sato, and W. Melnitchouk (Jefferson Lab Angular Momentum (JAM) Collaboration), Global QCD analysis of pion parton distributions with threshold resummation, Phys. Rev. Lett. **127**, 232001 (2021).

[26] G. R. Farrar and D. R. Jackson, Pion and nucleon structure functions near $x = 1$, Phys. Rev. Lett. **35**, 1416 (1975).

[27] E. L. Berger and S. J. Brodsky, Quark structure functions of mesons and the Drell-Yan process, Phys. Rev. Lett. **42**, 940 (1979).

[28] J. F. Gunion, P. Nason, and R. Blankenbecler, Power-suppressed contributions to deep-inelastic processes, Phys. Rev. D **29**, 2491 (1984).

[29] C. Leon and M. Sargsian, A non-perturbative model of mean field valence quarks, PoS **LC2019**, 056 (2020).

[30] C. Leon and M. Sargsian, Residual mean field model of valence quarks in the nucleon, Eur. Phys. J. C **82**, 309 (2022).

[31] R. Abir *et al.*, The case for an EIC theory alliance: Theoretical challenges of the EIC, arXiv:2305.14572.

[32] S. J. Brodsky, H.-C. Pauli, and S. S. Pinsky, Quantum chromodynamics and other field theories on the light cone, Phys. Rep. **301**, 299 (1998).

[33] Y. V. Kovchegov and E. Levin, *Quantum Chromodynamics at High Energy* (Cambridge University Press, Cambridge, 2012).

[34] G. Sterman, J. Smith, J. C. Collins, J. Whitmore, R. Brock, J. Huston, J. Pumplin, W.-K. Tung, H. Weerts, C.-P. Yuan, S. Kuhlmann, S. Mishra, J. G. Morfín, F. Olness, J. Owens, J. Qiu, and D. E. Soper, Handbook of perturbative QCD, Rev. Mod. Phys. **67**, 157 (1995).

[35] A. V. Belitsky and A. V. Radyushkin, Unraveling hadron structure with generalized parton distributions, Phys. Rep. **418**, 1 (2005).

[36] Z. Dziembowski and L. Mankiewicz, Light-meson distribution amplitude: Simple relativistic model, Phys. Rev. Lett. **58**, 2175 (1987).

[37] T. Huang, B.-Q. Ma, and Q.-X. Shen, Analysis of the pion wave function in the light-cone formalism, Phys. Rev. D **49**, 1490 (1994).

[38] B. Pasquini and P. Schweitzer, Pion transverse momentum dependent parton distributions in a light-front constituent approach, and the Boer-Mulders effect in the pion-induced Drell-Yan process, Phys. Rev. D **90**, 014050 (2014).
[39] A. P. Trawiński, Hadron light-front wave functions based on AdS/QCD duality, Ph.D. thesis, Warsaw University, 2016.
[40] A. P. Trawiński, The pion renormalized light-cone wave function, Few-Body Syst. **57**, 449 (2016).
[41] G. Lepage and S. J. Brodsky, Exclusive processes in perturbative quantum chromodynamics, Phys. Rev. D **22**, 2157 (1980).
[42] L. L. Frankfurt and M. I. Strikman, High-energy phenomena, short-range nuclear structure and QCD, Phys. Rep. **76**, 215 (1981).
[43] M. M. Sargsian and F. Vera, New structure in the deuteron, Phys. Rev. Lett. **130**, 112502 (2023).
[44] L. L. Frankfurt and M. I. Strikman, On the normalization on the spectral function of the nucleus and the EMC effect, Phys. Lett. B **183**, 254 (1987).
[45] R. L. Jaffe and A. Manohar, Deep inelastic scattering from arbitrary spin targets, Nucl. Phys. B **321**, 343 (1989).
[46] M. M. Sargsian, Large Q^2 electrodisintegration of the deuteron in the virtual nucleon approximation, Phys. Rev. C **82**, 014612 (2010).
[47] S. J. Brodsky, T. Huang, and G. P. Lepage, Hadronic wave functions and high momentum transfer interactions in quantum chromodynamics, in *Particles and Fields 2*, edited by A. Z. Capri and A. N. Kamal (Plenum Press, Banff, Canada, 1981).
[48] B. Pasquini and S. Rodini, The twist-three distribution $e^q(x, k_\perp)$ in a light-front model, Phys. Lett. B **788**, 414 (2019).
[49] C. Leon, M. M. Sargsian, and F. Vera, A novel feature of valence quark distributions in hadrons, Physics **3**, 913 (2021).
[50] J. Badier, J. Boucrot, J. Bourotte, G. Burgun, O. Callot, P. Charpentier, M. Crozon, D. Decamp, P. Delpierre, B. Gandois, R. Hagelberg, M. Hansroul, Y. Karyotakis, W. Kienzle, P. Dû, J. Lefrançois, T. Leray, J. Maillard, A. Michelini, P. Miné, *et al.* (NA3 Collaboration), Experimental J/ψ hadronic production from 150 to 280 GeV/c, Z. Phys. C - Particles and Fields **20**, 101 (1983).
[51] B. Betev, J. J. Blaising, P. Bordalo, A. Boumediene, L. Cerrito, A. Degré, A. Ereditato, S. Falciano, K. Freudenreich, E. Gorini, M. Guanziroli, H. Hofer, P. Juillot, L. Kluberg, P. Lecomte, P. Coultre, R. Morand, B. Mours, A. Romana, R. Salmeron, *et al.* (NA10 Collaboration), Differential cross-section of high-mass muon pairs produced by a 194 GeV/cπ^- beam on a tungsten target, Z. Phys. C - Particles and Fields **28**, 9 (1985).
[52] J. S. Conway, C. E. Adolphsen, J. P. Alexander, K. J. Anderson, J. G. Heinrich, J. E. Pilcher, A. Possoz, E. I. Rosenberg, C. Biino, J. F. Greenhalgh, W. C. Louis, K. T. McDonald, S. Palestini, F. C. Shoemaker, and A. J. S. Smith (E615 Collaboration), Experimental study of muon pairs produced by 252-GeV pions on tungsten, Phys. Rev. D **39**, 92 (1989).
[53] A. Candido, F. Hekhorn, and G. Magni, EKO: Evolution kernel operators, Eur. Phys. J. C **82**, 976 (2022).
[54] S. Navas, C. Amsler, T. Gutsche, C. Hanhart, J. J. Hernández-Rey, C. Lourenço, A. Masoni, M. Mikhasenko, R. E. Mitchell, C. Patrignani, C. Schwanda, S. Spanier, G. Venanzoni, C. Z. Yuan, K. Agashe, G. Aielli, B. C. Allanach, J. Alvarez-Muñiz, M. Antonelli, E. C. Aschenauer, *et al.* (Particle Data Group), Review of particle physics, Phys. Rev. D **110**, 030001 (2024).
[55] R. P. Feynman, Photon-hardon interations, *Frontiers in Physics* (CRC Press, 1998).